Chinese Journal of
POLYMER SCIENCE

RAPID COMMUNICATION

https://doi.org/10.1007/s10118-022-2829-7
Chinese J. Polym. Sci. **2022**, *40*, 1323–1330

Seamlessly-integrated Textile Electric Circuit Enabled by Self-connecting Interwoven Points

Hui-Yang Wu†, Xiang Shi†, Zi-Hao Zhou, Yue Liu, Xiang-Ran Cheng, Yi-Bei Yang, Xin-Yue Kang, Yue Guo, Kai-Wen Zeng, Bing-Jie Wang*, Xue-Mei Sun, Pei-Ning Chen*, and Hui-Sheng Peng*

State Key Laboratory of Molecular Engineering of Polymers, Laboratory of Advanced Materials and Department of Macromolecular Science, Fudan University, Shanghai 200438, China

Electronic Supplementary Information

Abstract Flexible, breathable and lightweight electronic textiles hold great promise to change the ways we intact with electronics. Electrical connections among functional components are indispensable for system integrations of electronic textiles. However, it remains challenging to achieve mechanically and electrically robust connections to fully integrate with interwoven architecture and weaving process of textiles. Here, we reported a seamlessly-integrated textile electric circuit by weaving conductive fibers with self-connecting capacity at the interwoven points. Self-connecting conductive fibers (SCFs) were prepared by coating modified polyurethane conductive composites onto nylon fibers. Electrical connections were achieved at interwoven points in less than 5 s once the weft and warp SCFs were woven together, due to the designed dynamic bonds of aromatic disulfide metathesis and hydrogen bonds in the modified polyurethane (MPU). The self-connecting point was electrically stable (varied by less than 6.7% in electrical resistance) to withstand repeated deformations of bending, pressing and even folding. Such a self-connecting strategy could be generalized to weave full-textile electronics capable of receiving signals and displaying with enhanced interfacial stability, offering a new way to unify fabrication of electronics and weaving of textiles.

Keywords Electronic textile; Electric circuit; Conductive fiber; Function integration

Citation: Wu, H. Y.; Shi, X.; Zhou, Z. H.; Liu, Y.; Cheng, X. R.; Yang, Y. B.; Kang, X. Y.; Guo, Y.; Zeng, K. W.; Wang, B. J.; Sun, X. M.; Chen, P. N.; Peng, H. S. Seamlessly-integrated textile electric circuit enabled by self-connecting interwoven points. *Chinese J. Polym. Sci.* **2022**, *40*, 1323–1330.

INTRODUCTION

The emergence of Internet of Things and 5G in the past decade have boosted rapid development of electronic textiles that are intrinsically flexible, breathable and lightweight to seamlessly fit irregular and soft human bodies, which are regarded as next-generation wearable electronics.[1–4] Electronic textiles with functionalities like displaying,[5,6] energy supplying,[7–9] sensing,[10–12] and computing[13–15] have been realized to offer promising opportunities to revolutionize the ways we interact with electronics. For practical applications, electric circuits are the indispensable building blocks to connect functional electronic textiles together to form a close-loop integration system. However, conventional electric circuits are generally made by directly patterning thin-film conductive paths on planar substrates through deposition or etching, which are intrinsically inapplicable to the weft-warp interwoven architecture and weaving process of textiles.[16–18] It is crucial while remains far less developed to achieve electric circuits that can seamlessly and stably integrate with textiles for wearable uses.

Weaving conductive fibers into textile is promising to realize electric circuits to well unify with textile architecture and manufacturing, in which conductive paths with designable patterns could be built in warp and weft directions.[19] Besides conductive paths, stable electrical connections among conductive fibers and/or electronic components are indispensable for complete electric circuits. Soldering is currently an optimal option to make connections for conventional integrated circuits, but its intrinsic rigidness and brittleness generally make the resultant electronic textiles functionally degrade or even fail under complex deformations. The high-temperature soldering process is also incompatible with the textile made of polymer fibers.[18,20] While conductive adhesives composed of metal particles and polymer resin matrix displayed superior flexibility to soldering materials, their weakness in interfacial strength with conductive fibers always leads to peeling off during repeated deformations. Moreover, the use of solvent-containing conductive adhesives generally causes low processing accuracy of electric cir-

* Corresponding authors, E-mail: wangbingjie@fudan.edu.cn (B.J.W.)
E-mail: peiningc@fudan.edu.cn (P.N.C.)
E-mail: penghs@fudan.edu.cn (H.S.P.)
† These authors contributed equally to this work.
Received May 10, 2022; Accepted June 24, 2022; Published online September 2, 2022

cuits due to their permeation in the textile.[18,21,22] It is still an unmet need for electronic textiles to realize mechanically and electrically reliable connections that fully integrate with interwoven architecture and weaving process.

Herein, we reported a seamlessly-integrated textile electric circuit by weaving conductive fibers with electrically self-connecting capacity at the interwoven points (Fig. 1a). Such conductive fibers, namely self-connecting fibers (SCFs), were prepared by coating modified polyurethane (MPU) composited with conductive components on nylon fibers. Upon weaving together warp and weft SCFs, stable electrical connection was automatically achieved at the interwoven points between SCFs in 5 s due to dynamic bonds of aromatic disulfide metathesis and hydrogen bonds in the MPU (Fig. 1b). Owing to the flexibility of composite MPU, the connecting points were stable and durable to withstand folding and 1000 times of bending and pressing. Using such self-connecting strategy, fully-integrated textile electric circuits were realized facilely without any traditional soldering operations. The MPU could also be used to fabricate stable full-textile electronics like textile displays.

EXPERIMENTAL

Materials

2,2-Bis(hydroxymethyl)propionic acid (DMPA, 98%) was ordered from Macklin. Poly(ethylene adipate) (PEA, with a molecular weight of 2000) was acquired from Aoke New Material Technology Co., Ltd. Isophorone diisocyanate (IPDI, 99%) and 4-aminophenyl disulfide (APDS, 98%) were purchased from Aladdin. 2-Hydroxyethyl disulfide (HEDS, technical grade) was purchased from Aldrich. Dibutyltin dilaurate (>95.0%) was purchased from Tokyo Chemical Industry (TCI, Japan). Triethylamine (TEA, ≥99%), ethylenediamine (EDA, analytical grade), dried *N*,*N*-dimethylformamide (DMF), dried tetrahydrofuran, and acetone were purchased from Sinopharm

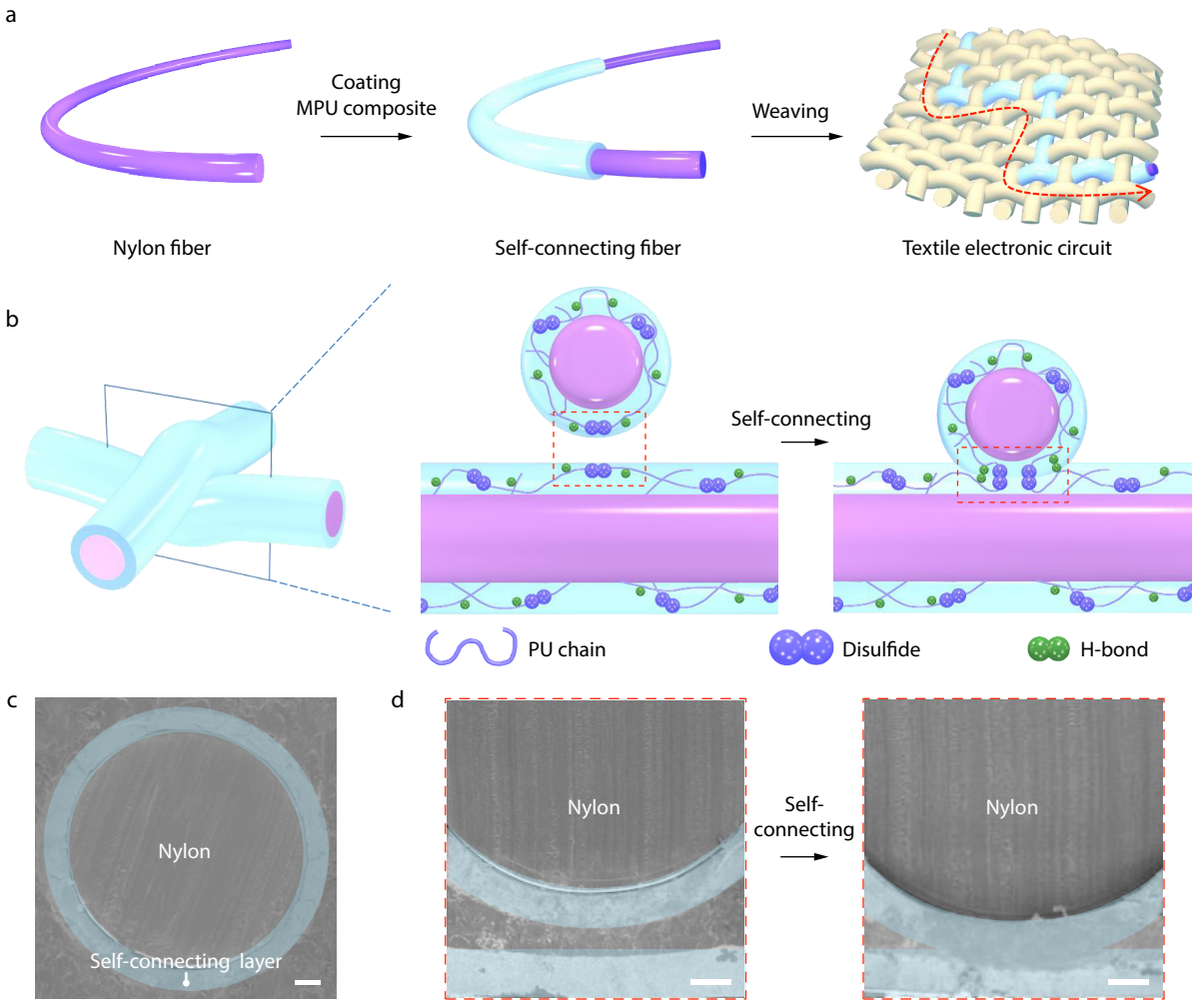

Fig. 1 Schematic and characteristics of textile electric circuits. (a) Schematic illustrating the fabrication of an SCF by coating MPU composite and a textile circuit by weaving SCFs. (b) The self-connecting process at the warp-weft interwoven point enabled by aromatic disulfide bonds and hydrogen bonds (urethane-urethane, urethane-urea, urea-urea) in the MPU. (c) Cross-sectional SEM images of an SCF. (d) Cross-sectional SEM images of the interface at the interwoven point between two SCFs before (left) and after (right) self-connecting. Scale bars in the (c) and (d): 30 μm. The self-connecting layer made of MPU/MWCNTs composite was marked with blue in the (c) and (d) to better identify.

https://doi.org/10.1007/s10118-022-2829-7

Chemical Reagent Co., Ltd. The MWCNT waterborne dispersion (13.8 wt%) was purchased from Chengdu Organic Chemicals Co., Ltd., Chinese Academy of Sciences.

Synthesis of MPU and HMPU Emulsions

For the synthesis of MPU emulsion, DMPA was dehydrated in an oven at 110 °C for 5 h. PEA (7.5 g) in a three-neck vessel was dried under vacuum at 120 °C for 4 h before cooling to 85 °C. DMPA (0.141 g) dissolved in 2 mL of dried DMF, IPDI (1.695 g) and dibutyltin dilaurate (0.138 g) were sequentially added and stirred for 6 h in an argon atmosphere under reflux condensation to be pre-polymerized. After cooling to 60 °C, 0.467 g of APDS dissolved in 2 mL of dried tetrahydrofuran was added to the above reaction system and stirred for additional 3 h for chain extension. Acetone (10 g) was then added to regulate the viscosity of the mixture during the reaction. Neutralization using TEA (0.111 g) was performed for 20 min below 40 °C. Finally, the mixture was emulsified by 10 mL of deionized water and 0.047 g of EDA at 1500 r/min for 30 min to obtain a homogenous MPU emulsion. To synthesize HMPU emulsion, APDS was replaced by HEDS, the amount of DMPA, PEA, IPDI, dibutyltin dilaurate, HEDS, TEA, deionized water and EDA was changed to 0.376 g, 7.5 g, 2.666 g, 0.138 g, 0.386 g, 0.284 g, 20 mL and 0.125 g, respectively. The processes of prepolymerization, chain extension, neutralization and emulsification were performed for 3 h, 3.5 h, 30 min and 30 min, respectively.

Preparation of the PU Films

The obtained emulsion was poured into Teflon molds and PU films were acquired by evaporating the solvent at 45 °C for 8 h, 60 °C for 3 h, and 70 °C in a vacuum oven for 2 h in turn.

Fabrication of Textile Circuits

The MWCNT waterborne dispersion was mixed with the PU emulsion with a weight ratio of 30%. After degassing in a vacuum oven, the liquid mixture was poured into rubber grooves with slits on the side. We designed sizes and arrangement of rubber grooves to pattern the MPU layer on fiber substrate. The nylon fibers were horizontally embedded into the slits to fully dip in the liquid mixture for 3 min, and then they were horizontally pulled out from the emulsion at a speed of ~5 mm/min, followed by drying in an air oven at 70 °C for 30 min to form SCFs. The SCFs with intermittent coating of MPU were cut into pre-designed segments (Fig. S5 in the electronic supplementary information, ESI), and then woven into textile and adjusted manually to ensure self-connected points formed at the pre-designed place.

Fabrication of Electroluminescent (EL) Textile

The fabrication method of the transparent conductive wefts and luminescent warps referred to the previous work.[6] MPU was dip-coated on conductive wefts and luminescent warps, followed by drying at 70 °C for 1 h. The individual EL unit was fabricated by interlacing luminescent warp fibers with conductive weft fibers. The EL textile array containing 64 EL units was fabricated by weaving transparent conductive wefts and luminescent warps with cotton yarns as well as other fiber materials like polyester and flax fibers. The density of transparent conductive wefts and the luminescent warps was 0.5 pick/cm and 1 end/cm, respectively.

Characterization

Morphology was obtained by scanning electron microscopy (SEM, Zeiss Gemini SEM500 FESEM operated at 2 kV). Fourier transform infrared (FTIR) spectrum was obtained from Fourier transform infrared spectrometer (Thermofisher, Nicolet 6700) and ^{1}H nuclear magnetic resonance (NMR) spectrum was obtained from a Bruker Advance 400 MHz spectrometer at room temperature. Mechanical properties were obtained from a universal testing instrument (HY-0580, Shanghai Hengyi Testing Instruments Co., Ltd.). Electrical performances were recorded by a CHI660E electrochemical station and a digital multimeter (VICTOR VC9807A+). The EL unit was driven by a function waveform generator (Keysight 33500B Series) and a high-voltage power amplifier (610E, TREK). The electromagnetic signal was generated by a function waveform generator (Keysight 33500B Series) and detected by an oscilloscope (Tektronix TDS 2012C). Photographs were obtained by a digital camera (D3400, Nikon). The pressing stability of textile circuit was tested by putting a 50 g object on the sample, and each press lasted for 2 s.

RESULTS AND DISCUSSION

As the building block for SCFs, MPU was synthesized using polyethyl dialcohol adipate as soft segment, 2,2-bis(hydroxymethyl)propionic acid as hydrophilic component, isophorone diisocyanate as hard segment, ethylenediamine as chain extender, and 4-aminophenyl disulfide (APDS) as bonding component.[23–25] The successful synthesis of MPU was verified by the characteristic bands at 3372 cm^{-1} ($\nu_{(-NH-)}$), 1727 cm^{-1} ($\nu_{(C=O)}$), and 1133 cm^{-1} ($\nu_{(C-O-C)}$) in the FTIR spectrum (Fig. S1 in ESI). The peaks at 6.50 and 7.06 ppm in the ^{1}H-NMR spectrum were assigned to aromatic ring protons in APDS that enabled metathesis of aromatic disulfides (Fig. S2 in ESI).[26–28] Especially, the functional groups of —NH—(C=O)—NH— and —O—(C—O)—NH— at 7.39 and 7.31 ppm rendered the hydrogen and oxygen for hydrogen bonds.[24] Metathesis of aromatic disulfides was essential for the self-connecting at room temperature, with the aid of dynamic interactions of hydrogen bonds among urethane-urethane, urethane-urea and urea-urea.[24]

Once two MPU films contacted with each other at room temperature, they were bound together in a few seconds due to the reversible reaction occurred at the interface. The resultant MPU film showed similar tensile stress (288 kPa) and breaking strain (1159%) to the original one (Fig. S3 in ESI). Such MPU was further endowed with electrical conductivity by compositing with conductive additives like multiwalled carbon nanotubes (MWCNTs) with a content of 30 wt%. MWCNTs were homogeneously dispersed in the MPU to form a continuous conductive network (Fig. S4 in ESI). The MPU/MWCNT composite was then dip-coated on the selected areas of nylon fibers to prepare SCFs (Fig. S5 in ESI). The resistances of an SCF (with length of 2 cm) were varied by less than 3% when it was bent with bending radii from 10 mm to 1 mm (Fig. S6a in ESI), and they also remained stable under repeated pressing tests (Fig. S6b in ESI). Typically, an SCF possessing a 30-μm-thick MPU/MWCNT composite layer was used unless specified in this study (Fig. 1c).

The electrical connecting occurred at the warp-weft inter-

https://doi.org/10.1007/s10118-022-2829-7

woven points as the SCFs were woven into a textile according to a pre-designed pattern and interlaced with each other (Fig. S5b in ESI). An individual connecting point between two interlaced SCFs was carefully investigated to evaluate the electrical and mechanical performances. The MPU/MWCNT composite layers on the interlaced SCFs were fused together without any obvious gap (Fig. 1d and Fig. S7 in ESI). The conductivity and mechanical strength of the self-connecting point are two important parameters for efficient electrical connecting. Due to the swift bonding formation at room temperature, once the SCFs contacted with each other, the resistance between SCFs sharply dropped from open circuit state to 2.2 kΩ in a short time of 0.2 s and then stably maintained (Fig. 2a). Such electrical connecting was mechanically robust even when the interwoven point (*i.e.*, fused MPU/MWCNT composite layer) was stretched in the opposite directions with a large strain of over 550% (Fig. 2b). The resistance of the self-connecting point varied by less than 4% when the interlaced fiber was sharply bent with a bending radius of 1 mm (Fig. 2c). Due to the flexibility and elasticity of the composite MPU, the electrical connecting state of the interwoven point was also well maintained after 1000 cycles of pressing (Fig. 2d). Moreover, because the MPU layer was chemically stable, the electrical connection could be achieved even after the

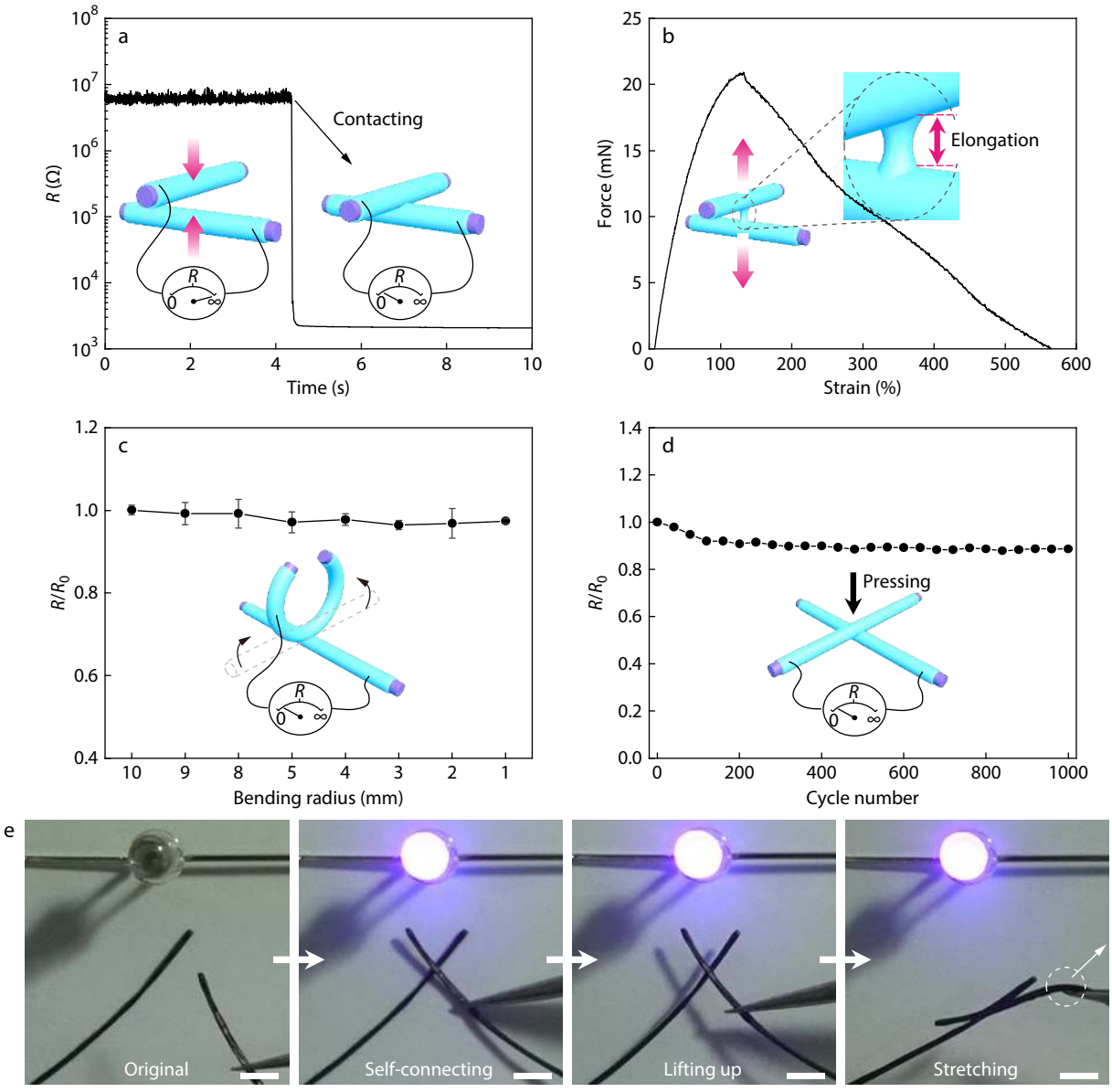

Fig. 2 Stable electrical connection at the interwoven point between two conductive fibers coated with MPU/MWCNT layer. (a) Electrical resistance variation when the interwoven SCFs contacted with each other. (b) Force-strain curve of the self-connecting point when SCFs were stretched in the opposite directions. Strain = D/D_0, D represents the distance between SCFs, and D_0 equals the thickness of the MPU/MWCNT layer. (c, d) Dependence of electrical resistance on bending radius of SCFs (c) and pressing cycle number (d). R_0 and R correspond to the electrical resistances before and after bending or pressing, respectively. (e) Photographs of a LED circuit in series with interlaced SCFs that were lifted and stretched. Scale bars in (e): 2 mm.

https://doi.org/10.1007/s10118-022-2829-7

SCFs were stored in open air for 3 months (Fig. S8 in ESI). We further tested the connecting stability in a circuit to light a LED (Fig. 2e). The LED was turned on immediately when the SCFs interlaced with each other, and the brightness of the LED stayed stable when the SCFs were lifted and stretched. Such electrical and mechanical robustness of the self-connecting point enabled by SCFs with MPU/MWCNT composite layer is crucial for the stable connecting of textile electronic circuits.

We further wove SCFs into cotton textile to obtain a textile electric circuit, in which the SCFs were interlaced with each other in weft and warp directions. The softness of the textile electric circuit could be well maintained after weaving with SCFs. The electrical connecting at the interwoven point formed in 5 s and was mechanically robust under stretching of textile (Fig. S9 in ESI). The connecting state was also maintained stably in the investigated 1000 cycles of bending (Fig. 3a). Moreover, the resistance of the textile circuit fluctuated by less than 4% even when the textile was folded (bent with 180°) along the middle lines and diagonal lines (Fig. S10 in ESI). As expected, when the woven SCFs in the textile circuit were further connected with a LED-driven circuit, no brightness variation was observed during the folding of textile (Fig. S11 in ESI). In comparison, for the textile circuit woven with conductive fibers based on conventional PU free of modified groups, its resistance fluctuated severely due to the interfacial instability at the interwoven point with poor contact between conductive fibers (Fig. 3a).

The mechanical properties of the MPU could be readily tuned to meet the demand for high tensile strength. For instance, a high-strength MPU (HMPU) was synthesized by increasing the ratio of hard segments and using 2-hydroxyethyl disulfide instead of APDS, which was verified by the FTIR spectrum (Fig. S12 in ESI).[23] After a thermal treatment at 70 °C for 2 h, the average strength of the HMPU was enhanced to over 18 MPa with a small relative standard devi-

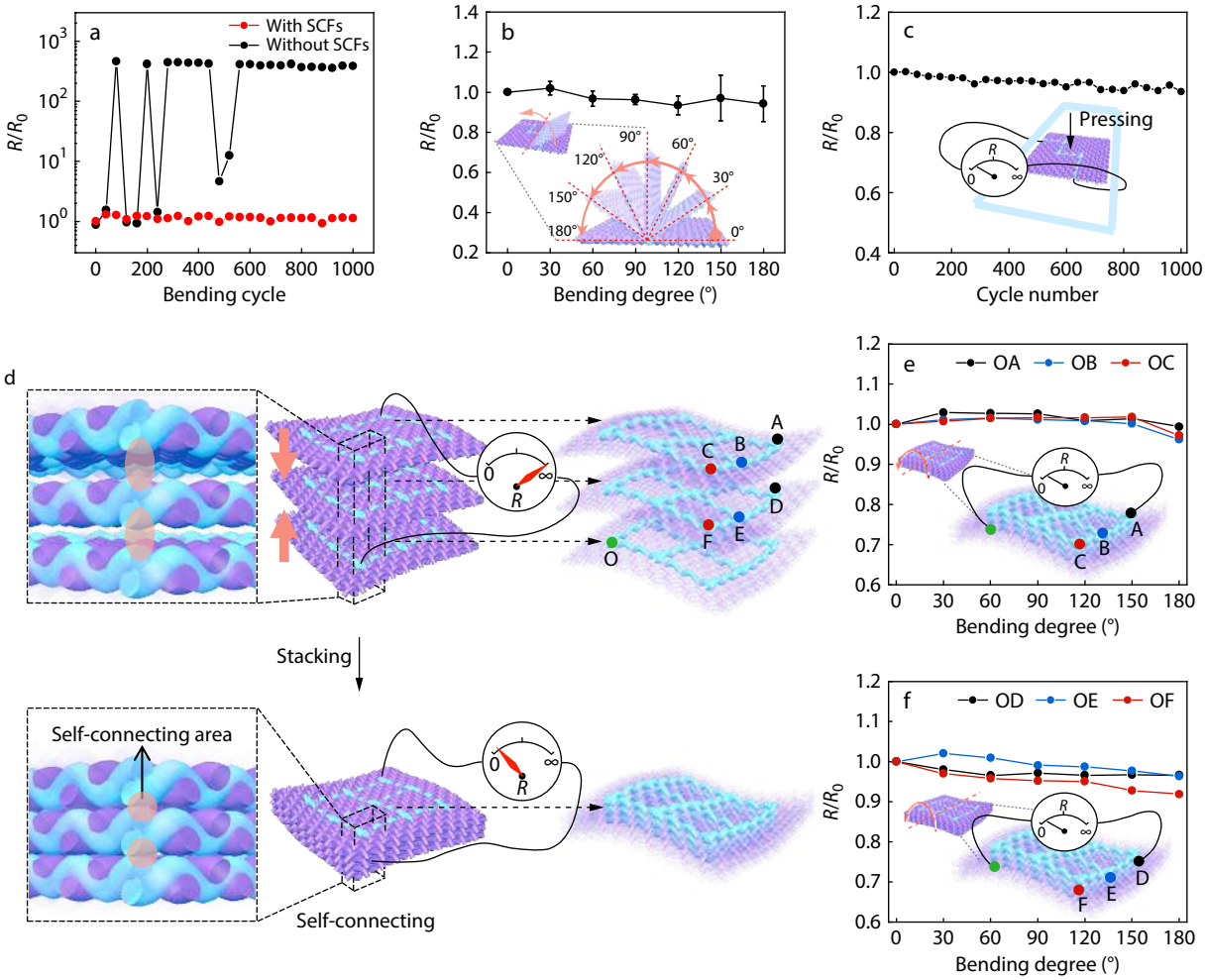

Fig. 3 Stability of self-connecting textile electric circuits. (a–c) Dependence of electrical resistance of the textile circuits on bending cycle (a), bending degree (b), and pressing cycle number (c). The bending degree in (a) is 60°. (d) Schematic illustration of the construction of a three-dimensional conductive network containing 27 connecting points. With electrical connecting between interwoven points in adjacent layers of textile (left inset), a conductive network was built in textile with electrically connecting points of A, B, C in the upper layer, D, E, F in the middle layer, and O in the underlayer (right inset). (e, f) Dependence of electrical resistance of OA, OB, OC (e), OD, OE, and OF (f) on bending angle. R_0 and R correspond to electrical resistances before and after bending or pressing, respectively.

https://doi.org/10.1007/s10118-022-2829-7

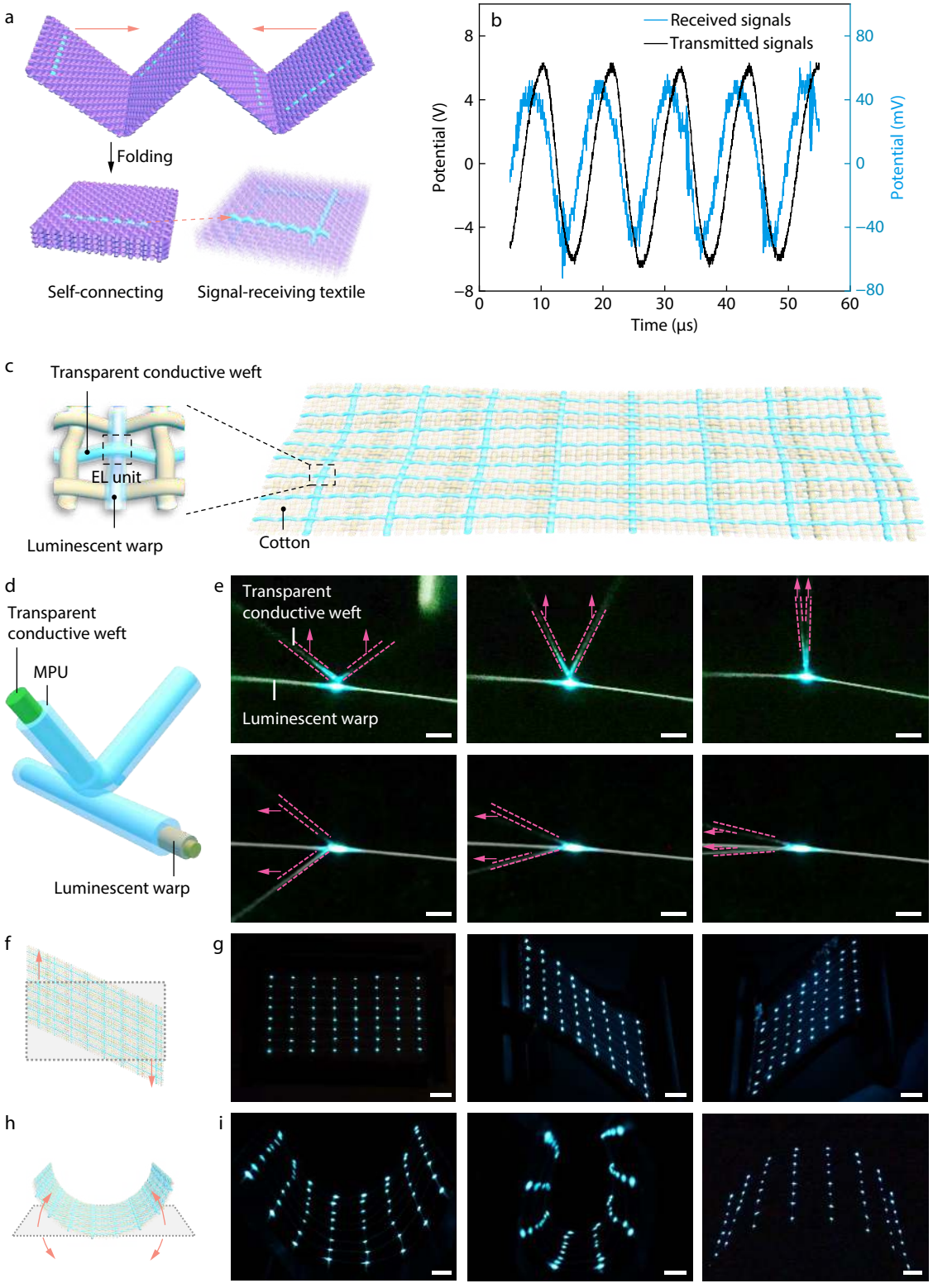

Fig. 4 Functional textile electronics based on SCFs. (a) Schematic showing the fabrication of a signal-receiving textile by folding in a zigzag arrangement to form a spiral coil. (b) The comparison of the received signals (blue) by the textile receiver coil and the transmitted signal (black) by a transmitter coil made of copper wires. (c) Schematic showing the weave diagram of the EL unit and textile array. (d) Structure of an EL unit. EL unit formed at the interwoven point between luminescent warp fibers and transparent conductive weft fibers. (e) Photographs of EL unit being stretched along vertical and horizontal directions. (f) Schematic and (g) photographs of the EL textile array being stretched. (h) Schematic and (i) photographs of the EL textile array being bent. Scale bars: (e) 3 mm, (g) 2 cm and (i) 1 cm.

https://doi.org/10.1007/s10118-022-2829-7

ation of less than 5.3% (Fig. S13 in ESI). The longer time for self-connecting was needed because the aliphatic disulfide in the HMPU had a lower metathesis reactivity than the aromatic disulfide in the MPU.[23,29] Besides MWCNTs, other conductive additives like nickel microparticles could also be incorporated in the HMPU to further enhance the conductivity. For instance, using the composite HMPU with a nickel microparticle content of 160 wt%, the resistance of a textile circuit with a self-connecting interwoven point was reduced to 10 Ω (Fig. S14 in ESI). Moreover, the strengths of the connecting points based on HMPU were 8.8 and 7.0 times higher than that based on MPU and conventional PU, respectively (Fig. S15 in ESI). As a result, stable electrical conducting was well maintained in the textile electric circuit under deformations (Fig. S16 in ESI). In comparison, drastic fluctuations occurred in the textile circuit without using SCFs.

For a typical electric circuit, conductive paths with multiple turning points are generally required to connect a lot of integrated electronic components. We wove a textile electric circuit having complex conductive paths with three turning points (Fig. S5c in ESI), which was electrically stable (varied by less than 6.7% in electrical resistance) during the folding and repeated pressing (Figs. 3b and 3c, and Fig. S17 in ESI). Furthermore, the electrical connection could also be built between adjacent stacked layers of textile electric circuits, making it possible to realize three-dimensional electronic textiles. Specifically, by stacking textile circuits containing 9 (3×3 array) self-connecting points, a three-dimensional conductive network containing 27 self-connecting points was obtained (Fig. 3d). The resistances of different conductive paths from point "O" to point "A–F" (Figs. 3e and 3f) varied by less than 5.3% during the bending test, indicating the robust electrical connection between the interwoven points.

The self-connecting strategy allowed to design a functional textile electronic system that seamlessly integrates with the textile interwoven architecture and weaving process. As a proof of concept, a signal-receiving textile circuit was fabricated by folding a four-layer textile in a zigzag arrangement (Fig. 4a), in which the woven SCFs were connected end to end to form spiral coils. The signal transmission was based on an electromagnetic introduction effect. When an alternating voltage was applied to a transmitter coil, the induced alternating magnetic field passed through the textile circuit to generate an alternating voltage output. Here we showed a sinusoidal signal generated from the transmitter coil could be completely received by this textile coil (Fig. 4b). The signal received by the textile coil based on SCFs was 5 times stronger than that by the counterpart without using SCFs (Fig. S18 in ESI). Such coils used to transfer signals were preferentially integrated with textiles to construct wearable electronics for healthcare.[30,31] Additionally, according to the applications, the chirality of the coil could be readily transferred by changing the way of folding (Fig. S19 in ESI).

Our textile circuit woven with SCFs was also suitable to seamlessly integrate with textile electronics to enable high interfacial stability under complex deformations. For instance, we built EL textile by weaving transparent conductive wefts and luminescent warps (Fig. 4c), in which ZnS phosphor served as the luminescent component.[6] When an alternating voltage was applied to the weft and warp fibers, in each ZnS phosphor particle at the weft-warp contact area, the generated electric field induces tunneling of holes and electrons from the conductive phase into ZnS lattice, and electrons and holes recombined to emit light once the electric field reversed. Each weft-warp interwoven point worked as an individual EL unit. The interfacial stability at the interwoven points directly determined the performances of the EL unit under deformations. By coating a layer of self-connecting MPU on the fibers, the weft-warp interwoven point could be effectively fixed by forming a stable contact interface, while the flexibility and breathability of the textile were well maintained (Fig. 4d). The resultant EL unit could stably work under various deformations such as stretching the conductive weft in different directions (Fig. 4e and Fig. S20 in ESI). As expected, the resultant EL textile containing 64 EL units (weave density of 2 ppi) showed uniform and stable brightness when the textile was repeatedly bent and stretched (Figs. 4f–4i and Fig. S21a in ESI). In contrast, a lot of EL units in textile based on a conventional PU layer failed under the bending and stretching deformations (Fig. S21b in ESI), due to the loose contact between conductive wefts and luminescent warps with a low weave density. The strategy based on self-connecting SCFs may provide a new thought for fully-integrated textile electronics.

CONCLUSIONS

In conclusion, a self-connecting strategy for textile electronic circuits is demonstrated by introducing dynamic bonds at the warp-weft contact interface of interlaced SCFs. The interfacial connections formed in 5 s at ambient conditions, which were mechanically robust and electrically stable under various complex deformations. By designing the weaving diagram of SCFs, textile electric circuits could be woven in a single layer and further assembled into a multi-layer architecture with high designability. The as-built textile electric circuit maintained stable electrical connections to withstand various deformations. Our strategy could also enable enhanced interfacial stability for textile electronics by modifying the fiber electrodes with self-connecting coatings. The self-connecting strategy offers a new way to develop fully-integrated textile electronics well compatible with interwoven structure and weaving process of textiles.

NOTES

The authors declare no competing financial interest.

Electronic Supplementary Information

Electronic supplementary information (ESI) is available free of charge in the online version of this article at http://doi.org/10.1007/s10118-022-2829-7.

ACKNOWLEDGMENTS

This work was financially supported by the National Natural

Science Foundation of China (Nos. 22175042, 52122310, 22075050 and 22105045), Science and Technology Commission of Shanghai Municipality (Nos. 20JC1414902, 21511104900 and 19QA1400800) and Shanghai Municipal Education Commission (No. 2017-01-07-00-07-E00062).

REFERENCES

1 Yang, Y.; Wei, X.; Zhang, N.; Zheng, J.; Chen, X.; Wen, Q.; Luo, X.; Lee, C. Y.; Liu, X.; Zhang, X.; Chen, J.; Tao, C.; Zhang, W.; Fan, X. A non-printed integrated-circuit textile for wireless theranostics. *Nat. Commun.* **2021**, *12*, 4876.

2 Lian, Y.; Yu, H.; Wang, M.; Yang, X.; Li, Z.; Yang, F.; Wang, Y.; Tai, H.; Liao, Y.; Wu, J.; Wang, X.; Jiang, Y.; Tao, G. A multifunctional wearable E-textile *via* integrated nanowire-coated fabrics. *J. Mater. Chem. C* **2020**, *8*, 8399–8409.

3 Ma, Y.; Ouyang, J.; Raza, T.; Li, P.; Jian, A.; Li, Z.; Liu, H.; Chen, M.; Zhang, X.; Qu, L.; Tian, M.; Tao, G. Flexible all-textile dual tactile-tension sensors for monitoring athletic motion during taekwondo. *Nano Energy* **2021**, *85*, 105941.

4 Wang, H.; Zhang, Y.; Liang, X.; Zhang, Y. Smart fibers and textiles for personal health management. *ACS Nano* **2021**, *15*, 12497–12508.

5 Zhang, Z.; Cui, L.; Shi, X.; Tian, X.; Wang, D.; Gu, C.; Chen, E.; Cheng, X.; Xu, Y.; Hu, Y.; Zhang, J.; Zhou, L.; Fong, H. H.; Ma, P.; Jiang, G.; Sun, X.; Zhang, B.; Peng, H. Textile display for electronic and brain-interfaced communications. *Adv. Mater.* **2018**, *30*, 1800323.

6 Shi, X.; Zuo, Y.; Zhai, P.; Shen, J.; Yang, Y.; Gao, Z.; Liao, M.; Wu, J.; Wang, J.; Xu, X.; Tong, Q.; Zhang, B.; Wang, B.; Sun, X.; Zhang, L.; Pei, Q.; Jin, D.; Chen, P.; Peng, H. Large-area display textiles integrated with functional systems. *Nature* **2021**, *591*, 240–245.

7 Li, Y.; Zhou, J.; Zhang, T.; Wang, T.; Li, X.; Jia, Y.; Cheng, J.; Guan, Q.; Liu, E.; Peng, H.; Wang, B. Highly surface-wrinkled and n-doped CNTs anchored on metal wire: a novel fiber-shaped cathode toward high-performance flexible Li-CO_2 batteries. *Adv. Funct. Mater.* **2019**, *29*, 1808117.

8 Xu, J.; Ding, J. N.; Zhou, X. S.; Zhang, Y.; Zhu, W. J.; Liu, Z. F.; Ge, S. H.; Yuan, N. Y.; Fang, S. L.; Baughman, R. H. Enhanced rate performance of flexible and stretchable linear supercapacitors based on polyaniline@Au@carbon nanotube with ultrafast axial electron transport. *J. Power Sources* **2017**, *340*, 302–308.

9 Yu, Z.; Li, L.; Zhang, Q.; Hu, W.; Pei, Q. Silver nanowire-polymer composite electrodes for efficient polymer solar cells. *Adv. Mater.* **2011**, *23*, 4453–4457.

10 Li, Z.; Wang, Z. Air/liquid-pressure and heartbeat-driven flexible fiber nanogenerators as a micro/nano-power source or diagnostic sensor. *Adv. Mater.* **2011**, *23*, 84–89.

11 Lee, J.; Kwon, H.; Seo, J.; Shin, S.; Koo, J. H.; Pang, C.; Son, S.; Kim, J. H.; Jang, Y. H.; Kim, D. E.; Lee, T. Conductive fiber-based ultrasensitive textile pressure sensor for wearable electronics. *Adv. Mater.* **2015**, *27*, 2433–2439.

12 Wang, H.; Liu, Z.; Ding, J.; Lepro, X.; Fang, S.; Jiang, N.; Yuan, N.; Wang, R.; Yin, Q.; Lv, W.; Liu, Z.; Zhang, M.; Ovalle-Robles, R.; Inoue, K.; Yin, S.; Baughman, R. H. Downsized sheath-core conducting fibers for weavable superelastic wires, biosensors, supercapacitors, and strain sensors. *Adv. Mater.* **2016**, *28*, 4998–5007.

13 Lee, J. B.; Subramanian, V. Weave patterned organic transistors on fiber for E-textiles. *IEEE T. Electron. Dev.* **2005**, *52*, 269–275.

14 Xu, X.; Zhou, X.; Wang, T.; Shi, X.; Liu, Y.; Zuo, Y.; Xu, L.; Wang, M.; Hu, X.; Yang, X.; Chen, J.; Yang, X.; Chen, L.; Chen, P.; Peng, H. Robust DNA-bridged memristor for textile chips. *Angew. Chem. Int. Ed.* **2020**, *59*, 12762–12768.

15 Wang, T.; Meng, J.; Rao, M.; He, Z.; Chen, L.; Zhu, H.; Sun, Q.; Ding, S.; Bao, W.; Zhou, P.; Zhang, D. Three-dimensional nanoscale flexible memristor networks with ultralow power for information transmission and processing application. *Nano Lett.* **2020**, *20*, 4111–4120.

16 Xu, F.; Wei, B.; Li, W.; Liu, J.; Liu, W.; Qiu, Y. Cylindrical conformal single-patch microstrip antennas based on three dimensional woven glass fiber/epoxy resin composites. *Compos. Part B Eng.* **2015**, *78*, 331–337.

17 Xu, F.; Qiu, Y. Simulation and electromagnetic performance of cylindrical two-element microstrip antenna array integrated in 3D woven glass fiber/epoxy composites. *Mater. Des.* **2016**, *89*, 1048–1056.

18 Agcayazi, T.; Chatterjee, K.; Bozkurt, A.; Ghosh, T. K. Flexible interconnects for electronic textiles. *Adv. Mater. Technol.* **2018**, *3*, 1700277.

19 Zhang, Y.; Wang, H.; Lu, H.; Li, S.; Zhang, Y. Electronic fibers and textiles: recent progress and perspective. *iScience* **2021**, *24*, 102716.

20 Post, E. R.; Orth, M.; Russo, P. R.; Gershenfeld, N. E-broidery: design and fabrication of textile-based computing. *IBM Syst. J.* **2000**, *39*, 840–860.

21 Cui, H.; Li, D.; Fan, Q. Reliability of flexible electrically conductive adhesives. *Polym. Adv. Technol.* **2013**, *24*, 114–117.

22 Cui, H.; Fan, Q.; Li, D. Surface functionalization of micro silver flakes and their application in electrically conductive adhesives for electronic package. *Int. J. Adhes. Adhes.* **2014**, *48*, 177–182.

23 Rekondo, A.; Martin, R.; de Luzuriaga, A. R.; Cabanero, G.; Grande, H. J.; Odriozola, I. Catalyst-free room-temperature self-healing elastomers based on aromatic disulfide metathesis. *Mater. Horiz.* **2014**, *1*, 237–240.

24 Zhang, M.; Zhao, F.; Luo, Y. Self-healing mechanism of microcracks on waterborne polyurethane with tunable disulfide bond contents. *ACS Omega* **2019**, *4*, 1703–1714.

25 Guo, H.; Han, Y.; Zhao, W.; Yang, J.; Zhang, L. Universally autonomous self-healing elastomer with high stretchability. *Nat. Commun.* **2020**, *11*, 2037.

26 Sarma, R. J.; Otto, S.; Nitschke, J. R. Disulfides, imines, and metal coordination within a single system: interplay between three dynamic equilibria. *Chem. Eur. J.* **2007**, *13*, 9542–9546.

27 Belenguer, A. M.; Friscic, T.; Day, G. M.; Sanders, J. K. M. Solid-state dynamic combinatorial chemistry: reversibility and thermodynamic product selection in covalent mechanosynthesis. *Chem. Sci.* **2011**, *2*, 696–700.

28 Aguirresarobe, R. H.; Martin, L.; Fernandez-Berridi, M. J.; Irusta, L. Autonomic healable waterborne organic-inorganic polyurethane hybrids based on aromatic disulfide moieties. *Express Polym. Lett.* **2017**, *11*, 266–277.

29 Xu, W. M.; Rong, M. Z.; Zhang, M. Q. Sunlight driven self-healing, reshaping and recycling of a robust, transparent and yellowing-resistant polymer. *J. Mater. Chem. A* **2016**, *4*, 10683–10690.

30 Micus, S.; Padani, L.; Haupt, M.; Gresser, G. T. Textile-based coils for inductive wireless power transmission. *Appl. Sci.* **2021**, *11*, 4309.

31 Fobelets, K.; Thielemans, K.; Mathivanan, A.; Papavassiliou, C. Characterization of knitted coils for E-textile. *IEEE Sens. J.* **2019**, *19*, 7835–7840.

https://doi.org/10.1007/s10118-022-2829-7